MRS Communications

https://doi.org/10.1557/s43579-024-00628-2

MRS Communications

Early Career Distinguished Presenter Research Letter

Beneath the disorder: Unraveling the impacts of doping on organic electronics and thermoelectrics

Andrew Tolton, Zlatan Akšamija, Department of Materials Science and Engineering, University of Utah, Salt Lake City, UT 84112, USA
Address all correspondence to Zlatan Akšamija at **zlatan.aksamija@utah.edu**

(Received 16 April 2024; accepted 14 August 2024)

Abstract

Organic materials have found widespread applications but require doping to overcome their intrinsically low carrier concentration. Doping injects free carriers into the polymer, moving the position of the Fermi level, and creates coulombic traps, changing the shape of the electronic density of states (DOS). We develop equations to explicitly map the DOS parameters to the Seebeck vs conductivity relationship. At low carrier concentrations, this relationship is a universal slope $-k_B/q$, while at higher carrier concentrations, the slope becomes dependent on the shape of the DOS. We conclude that, at high doping, a heavy-tailed DOS leads to higher thermoelectric power factors.

Introduction

Since their conception, organic electronics have been an exciting developmental technology. They are flexible, environmentally friendly compared to inorganic semiconductors, and they can be solution processed, which makes them relatively cheap to manufacture. Organics are, therefore, uniquely suited for scalable and innovative electronics. Because of this, they have been studied for several applications including photovoltaics, wearable electronics, and OLEDs, of which several have already reached the market. One promising developing application for organic electronics is organic thermoelectric devices.[1] Several polymers across the literature have been reported as having high Seebeck coefficients (S) and electrical conductivities (σ),[2] giving hope that polymers could be made with high thermoelectric conversion efficiency, which is dependent on the power factor $PF = \sigma S^2$. And yet high power factors have remained elusive as there is a tradeoff between S and σ.[3] This tradeoff is controlled by carrier concentration, which has opposing effects on the two—increasing carrier concentration typically increases conductivity but reduces the Seebeck coefficient.

Conjugated polymers have low intrinsic carrier concentrations and, thus, conductivities,[4] making doping necessary to introduce free carriers and improve conductivity. However, the coulombic effects of dopant counterions additionally create structural and energetic changes in the polymer, altering the shape of the electronic density of states (DOS), widening the DOS and incurring band tails.[5] This widening is characterized by dopant-induced disorder (DID), which creates trap states, reducing both carrier mobility and the Seebeck coefficient, lowering the PF.[6] Crucial to attaining high power factors is a robust understanding of the relationship between the DOS and the charge transport properties of conjugated polymers, captured by the S vs σ curve. The relationship between S and σ has been studied extensively in the literature, and several different behaviors have been observed, including $S \propto \ln(\sigma)$,[7] and $S \propto \sigma^{-1/4}$.[8,9] Several models have been proposed to explain these behaviors, such as the Kang-Snyder model which posits that $S \propto \sigma^{-1/s}$ where s is related to the exponent of the transport distribution function $\sigma_\mu(E) \propto E^s$.[10] However, these models often require values as large as $s = 10$ to fit some measurements,[11] which cannot be related to any physical properties of the polymer and may require varying parameter values across the S vs σ curve.[12] To overcome limitations imposed by DID, we need a physically interpretable mapping between the DOS and transport.

In this work, we relate the shape of the S vs σ curve to the properties of the DOS. We use the generalized Gaussian disorder model to parameterize the DOS using a fixed width Γ_E and shape parameter p. For each DOS, we vary the free-carrier concentration (n) and compute the corresponding Fermi level E_F and then simulate transport by solving the Pauli master equation to find S and σ for each combination of DOS parameters and carrier concentration. We find distinct behaviors in the S vs σ curve between high and low carrier concentrations, dependent on the behaviors of E_F and E_T. At low carrier concentrations, E_T is far from E_F and independent of n. In this regime, we find $S \propto -\frac{k_B}{q}\ln(\sigma)$, with a universal slope $\frac{-k_B}{q}$ consistent with some literature but having an offset dependent on Γ_E and p. At high carrier concentrations, E_T is close to E_F and transport is described by the Mott formula. Here, the S vs σ curve has a slope that depends on both the shape parameter p and the Γ_E. We conclude that to optimize the power factor, a high p value is needed at low Γ_E but a low p value is needed at high Γ_E. Therefore, when doping increases energetic disorder, a heavy-tailed DOS is favorable because it leads to a flatter S vs σ curve. By considering both the shape and the width of the DOS, we see a new avenue toward more efficient thermoelectrics.

Methods

To decouple the effects of DID and carrier concentration, we first simulate hopping transport, depicted schematically in Fig. 1(a), at varying carrier concentrations in a polymer with a fixed DOS. We model the DOS using the generalized Gaussian disorder model (GGDM), which parameterizes the DOS as follows

$$g(E) = 2N_0 \frac{pA(p)}{2\Gamma_E \xi(1/p)} exp\left\{-\left[\frac{A(p)|E|}{\Gamma_E}\right]^p\right\}, \qquad (1)$$

where N_0 is half of the total number of available sites, $A(p) = \sqrt{\xi(3/p)/\xi(1/p)}$, and ξ is the gamma function. The width of the DOS increases with the energetic disorder (Γ_E), and the shape varies with shape parameter p from Gaussian to exponential as p decreases from 2 to 1, as depicted in Fig. 1(b). To understand the effects of the DOS parameters on transport, we simulated transport using a series of different DOS curves with varying Γ_E and p.

We then used Pauli's master equation $\frac{dP_i}{dt} = 0 = \sum_j [W_{ij}P_i(1-P_j) - W_{ji}P_j(1-P_i)]$ to calculate Marcus hopping within a simulation space of $41 \times 41 \times 47$ different energy sites, where $W_{ij} = \frac{\nu_0}{\sqrt{4\pi E_0 k_B T}} \exp\left(-\frac{(E_0+\Delta E)^2}{4E_0 k_B T}\right)$ gives the rate at which an electron hops from site i to site j. E_0 is the Marcus polaronic activation energy, and ΔE is the energy difference between sites. Pauli's master equation is solved for the site occupation probabilities using a non-linear iterative solver. The rates were then used to simulate carrier transport in the polymer and extract the Seebeck coefficient, macroscopic conductivity, and carrier mobility as described Supplemental Information, Sect. S1.[13] The hopping probabilities were used to calculate carrier hopping rates for a polymer with a temperature of 300 K, a Marcus polaronic activation energy of 0.1 eV, and under an electric field of 10^5 V/m.

When we vary the carrier concentration without altering the parameters of the GGDM, we add carriers without changing the shape of the DOS—an increase carrier concentration simply increases the Fermi level and transport energy. The Fermi level was iteratively calculated so that $\int g(E)f(E)\mathrm{d}E = n$ where n is the concentration of free carriers, $g(E)$ is the DOS, and $f(E)$ is the Fermi function, as depicted in Fig. 1(b). The transport

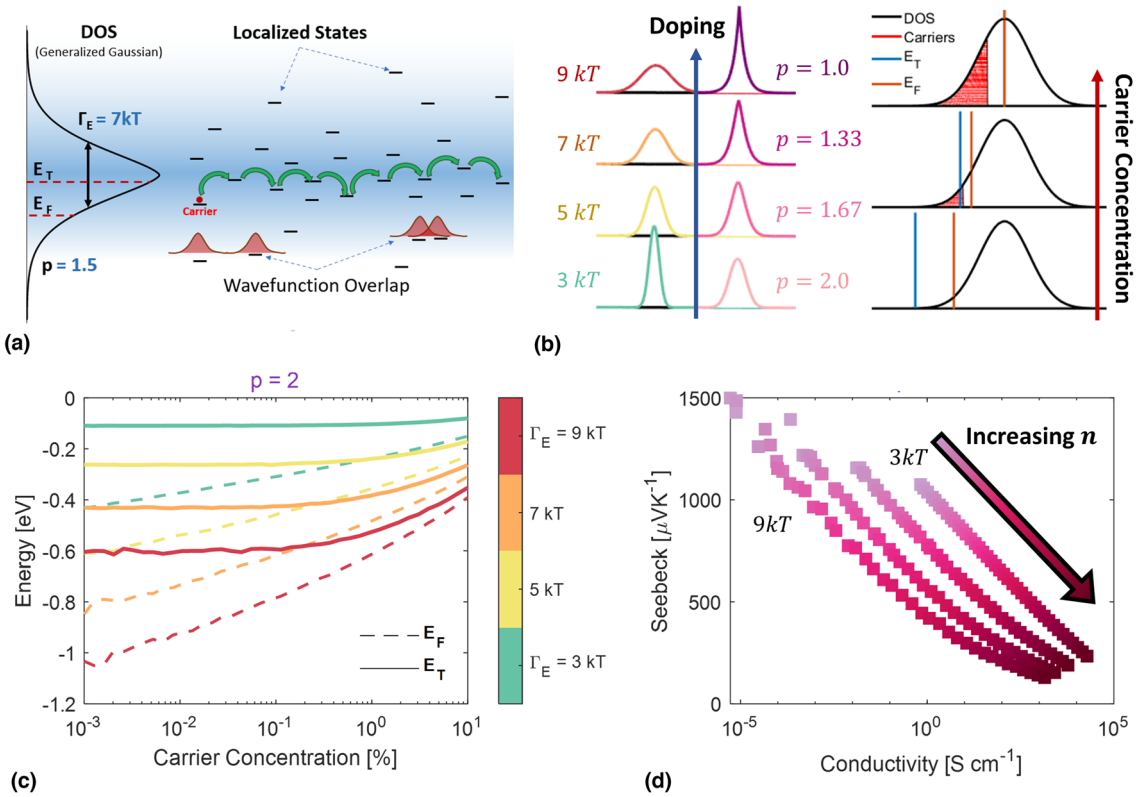

Figure 1. (a) Visualization of carriers hopping between localized energy sites with an energy distribution dictated by the density of states. The density of states is characterized by a generalized Gaussian with standard deviation Γ_E and shape parameter p. (b) (Left) Effects of Γ_E and p on the shape of the DOS. When a material is doped, it increases Γ_E and decreases p. (Right) To better understand the effect of Γ_E and p on transport, we vary the carrier concentration across each DOS without doping. This changes the Fermi level and transport energy without changing the shape of the DOS. (c) High and low carrier concentrations can be distinguished by looking at the $E_F(n)$ and $E_T(n)$ curves. At low carrier concentrations, E_T is independent of n and is far from E_F. At very high carrier concentrations, E_T and E_F are close and almost parallel. Moderate carrier concentrations follow a continuum between these extrema. (d) Seebeck vs conductivity for various energetic disorders from 3 to 9 kT at room T. At low n, the S vs σ curves appear parallel, but they start to curve with doping at different rates depending on the energetic disorder and p value.

energy is defined as $E_T = \frac{\int E\sigma_\mu(E)\mathrm{d}E}{\int \sigma_\mu(E)\mathrm{d}E}$ where E is energy and σ_μ is the transport distribution function and can qualitatively be understood as the average energy of transporting carriers. To find the Seebeck coefficient, we first calculate the Fermi level and transport energy, and then use the relationship $S = -\frac{1}{qT}(E_T - E_F)$. See Supplemental Information, Sect. S1, for more details on the calculations of the transport energy and Fermi level.

To analyze the effects of DID on transport, we numerically calculated the DOS to include Coulomb interactions between carriers and dopants according to the Arkhipov model, as described in our recent work.[5] We used the Arkhipov model to compute the DOS as a function of doping across a broad range of doping concentration, which was subsequently used to simulate hopping transport as described above. To analyze the impact of DID on the DOS, we compare the dopant-induced DOS with the GGDM and extract the Γ_E, the standard deviation of the DOS, using $\Gamma_E^2 = \int E^2 g(E)\mathrm{d}E / \int g(E)\mathrm{d}E$. For a given DOS, p was found by solving $M_{2p}/M_p^2 - (1+p) = 0$ using a secant method, where M_r is the rth absolute moment of the DOS.[14] A minimum dopant carrier separation of 0.3 nm and a dopant diameter of 0.2 nm were used when calculating the coulombic interactions between carrier and dopant counter-ion. Our model can capture a wide range of polymers and dopants, including capturing dopant size and spacing; however, our starting point here is a set of parameters consistent with our recent work that compared our calculations with measurements on P3HT, a widely used semiconducting conjugated polymer with high carrier mobility, doped with iodine.[5] Our terminology is summarized in Table S1 in Sect. S1 of the Supplemental Information.

Results and discussion

To understand the effects of the DOS parameters Γ_E and p on the S vs σ curve, we parameterized $S(\sigma, \Gamma_E, p)$. Our overall strategy is as follows: We started by parameterizing $E_F(n)$ and $\mu(n)$ and substituting these into the definition of conductivity $\sigma = q\mu n$. These terms rely on the parameter γ, which we defined as the exponent of $\sigma \propto n^\gamma$ and which we express in terms of Γ_E and p. We then relate E_F and σ and substitute into known expressions for $S(E_F)$, giving us a parameterization for $S(\sigma)$.

We begin by examining the S vs σ curve over a large range of carrier concentrations, where we observe distinct transport behaviors. These behaviors are delineated by the relationship of the Fermi Level E_F and transport energy E_T in response to carrier injection. We first analyze low carrier concentrations in the range of 0.001–0.1%. At these low carrier concentrations, the transport energy is constant and independent of the free-carrier concentration. Additionally, the Fermi level and transport energy are relatively well separated because the Seebeck coefficient is high. In contrast, at high carrier concentrations ($10-25\%$), the Fermi level and transport energy are very close, and the Seebeck coefficient is relatively small. Unlike at low carrier concentrations, the transport energy is a function of n in this range. We see from Fig. 1(c) that the response of the Fermi level and transport energies to free-carrier injection depend on the energetic disorder and p value, which is also reflected by the S vs σ curves in Fig. 1(d). This means that the distinction between "low doping" and "high doping" is disorder dependent, such that two different polymers at the same doping concentrations may have different S vs σ behavior, which may explain some of the disagreement in the literature when comparing polymers with different intrinsic disorder.

As is seen in Fig. 1(d), at low n, the S vs σ curves are parallel regardless of the energetic disorder Γ_E or shape parameter p. This gives us a hint about the form of the S vs σ relationship—the slope is independent of energetic disorder and p value and $S \propto \ln(\sigma)$. We use this observation to develop an expression for S vs σ using the strategy discussed above. We start by analyzing carrier mobility μ in terms of n, shown in Fig. 2(a). We find that μ vs n is linear on a log–log plot, indicating a power-law relationship of the form:

$$\mu = \mu_{\mathrm{sat}}(\Gamma_E)\left(\frac{n}{N_0}\right)^{\gamma-1}, \tag{2}$$

where μ_{sat} is defined as the maximum mobility achievable by a polymer with a given energetic disorder. This power-law dependence had been noted before in the literature, but the exponent and intercept had not been connected to the shape of the DOS. μ_{sat} is the saturation mobility, found at high carrier concentrations, and will be discussed in a later section.

The Fermi Level as a function of free-carrier concentration is plotted in Fig. 2(a), where we observe a linear relationship, indicating a logarithmic relationship that we fit by

$$E_F = \gamma k_B T ln\left(\frac{n}{N_0}\right) - 1.75\Gamma_E. \tag{3}$$

The slope of E_F is proportional to γ, which we realized knowing that γ must cancel out of the E_F vs σ relationship for the S vs σ lines to be parallel. Equation 3 has excellent agreement with the data, and the appearance of γ in the slope of $E_F(n)$ suggests that γ is a fundamental transport parameter that encapsulates the properties of the DOS. We also find the empirical relationship for the exponent

$$\gamma - 1 \approx 25(\Gamma_E - k_B T)^p \tag{4}$$

by extracting the slope of the μ vs n curve on a log–log scale, and the results of this fit are shown in Supplemental Information, Sect. S2.

Solving for $n(E_F)$ and substituting into $\sigma = q\mu n$, we get the dependence of conductivity on carrier concentration and DOS parameters $\sigma = q\mu_{\mathrm{sat}} N_0 \left(\frac{n}{N_0}\right)^\gamma$. Rearranging this to solve for E_F, we get the expression:

$$E_F = k_B T ln\left(\frac{\sigma}{\sigma_{\mathrm{sat}}}\right) - 1.75\Gamma_E, \tag{5}$$

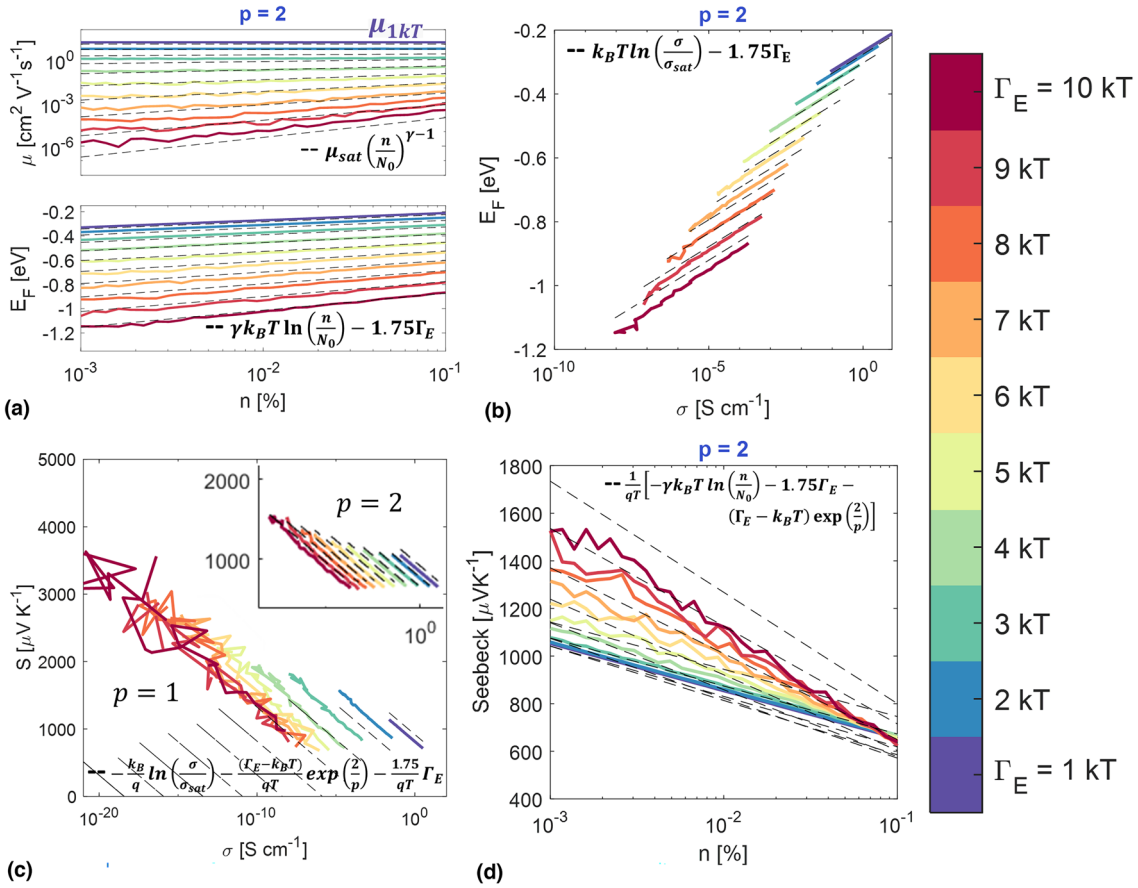

Figure 2. (a) (Top) Mobility vs carrier concentration at $p = 2$. The top line is mobility at $\Gamma_E = 1kT$, which we define as μ_{1kT} so that $\mu_{sat} = kT \cdot \mu_{1kT}/\Gamma_E$. μ_{sat} is relatively independent of p, and we use it to approximate mobility as $\mu \approx \mu_{sat}\left(\frac{n}{N_0}\right)^{\gamma-1}$ which shows good agreement. (Bottom) The Fermi level is proportional to the doping concentration, and the slope is surprisingly also dependent on γ. (b) At low carrier concentrations, γ dependence of the mobility and Fermi level cancels out such that the E_F vs σ curves are parallel. This is ultimately what gives us parallel S vs σ curves. (c) S vs σ at $p = 2$ (inset) and at $p = 1$, main fig, along with our approximation for S vs σ shown by the dashed lines. Using this approximation, we get a fantastic fit for S vs σ at low carrier concentrations and high p values, which is the relevant range for low doping concentrations. (d) Looking at S vs n, we see that for a constant energetic disorder and p value, the S vs n slope is constant, but in general, the slope of S vs n depends on γ and, thus, Γ_E and p.

where the saturation conductivity is related to saturation mobility through $\sigma_{sat} = q\mu_{sat}N_0$. Notice that γ from the exponent of mobility cancels with γ from the slope of the Fermi Level, making the E_F vs σ curves parallel as seen in Fig. 2(b).

Finally, we find that we can approximate the transport energy as a constant dependent only on the DOS parameters, such that

$$E_T \approx -(\Gamma_E - k_B T)exp\left(\frac{2}{p}\right). \quad (6)$$

Equation 6 gives excellent agreement with hopping transport simulations, as shown in Supplemental Information, Sect. S3. Combining Eqs. 5 and 6 with the definition of the Seebeck coefficient $S = \frac{1}{qT}(E_F - E_T)$, we can put everything together to obtain

$$S = -\frac{k_B}{q} ln\left(\frac{\sigma}{\sigma_{sat}}\right) - \frac{(\Gamma_E - k_B T)}{qT} exp\left(\frac{2}{p}\right) - \frac{1.75}{qT}\Gamma_E. \quad (7)$$

Our expression in Eq. 7 predicts a universal slope of $-k_B/q$ for S vs $\ln(\sigma)$, which has been observed in the literature for low carrier concentrations[10,15] and is observed in our data in Fig. 2(c). To better understand Eq. 7, Fig. 2(c) shows the simulated S vs σ curves and the approximations given by Eq. 7 as we increase Γ_E and p. The S vs σ curve shifts left as Γ_E increases and shifts toward the bottom right as p increases. We see that Eq. 7 gives nearly flawless agreement the data at $p = 2$ but deviates at $p = 1$ at high energetic disorders. It seems that for higher p values, there is a regular Γ_E-dependent spacing, but at low p values, the S vs σ curves merge into each other and converge in a way Eq. 7 fails to account for. However, as discussed later, most polymers will still have high p values and low energetic disorders at low doping, at which Eq. 7 predicts S vs σ almost perfectly.

We can also relate the Seebeck to the carrier concentration by combining Eqs. 4 and 6 to reach

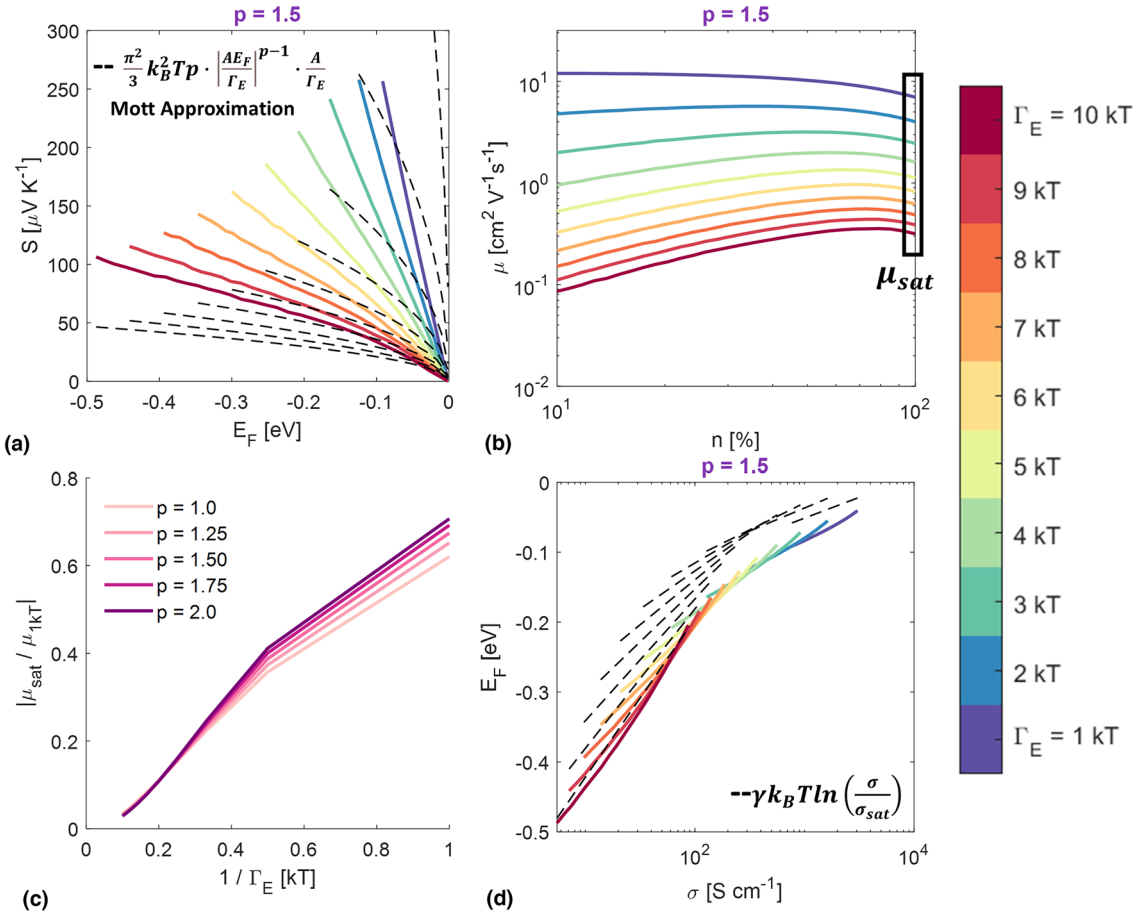

Figure 3. (a) The expression for $S(E_F)$ given by the Mott Formula works gives a decent qualitative fit at high n for polymers at moderate p values and high energetic disorders, which are the values we expect at high doping. (b) Compared to low carrier concentrations, the mobility is relatively independent of n at high carrier concentrations. We call the final mobility the saturation mobility, which is shown for multiple values of Γ_E and $p = 1.5$. (c) We see that the saturation mobility is nearly linear in $1/\Gamma_E$ and relatively independent of p, varying only by a factor<2. (d) The slope of $E_F(\sigma)$ is well captured by γ at high carrier concentrations, before the Seebeck nosedive which is omitted for visibility.

$S(n) = \frac{1}{qT}\left[-\gamma k_B T \ln\left(\frac{n}{N_0}\right) - 1.75\Gamma_E - (\Gamma_E - k_B T)\exp\left(\frac{2}{p}\right)\right]$, which is shown in Fig. 2(d) as dashed lines alongside hopping transport results. We see that the slope of $S(n)$ is proportional to γ, meaning that, in general, the slope depends on the energetic disorder and p value. Polymers in the disorder-free limit, however, should have a constant slope of $-k_B/q$ as has been observed in the literature.[16,17]

At high carrier concentrations, the Fermi level approaches the transport energy and the assumptions for the Mott formula become valid.[18] The Mott formula is given by $S = -\frac{\pi^2}{3}\frac{k_B^2 T}{q}\frac{d\ln\sigma_\mu}{dE}$ where σ_μ is the transport distribution function (TDF). From the generalized Einstein relation, we express the TDF as $\sigma_\mu = q^2 g(E) D(E)$. Because the microscopic diffusivity $D(E)$ is relatively weakly varying with carrier concentrations, we can replace it with a constant D_0 which disappears in the Mott Formula once we take the logarithmic derivative. Substituting the generalized Gaussian DOS from Eq. 1 into the Mott Formula, we get

$$S \approx \frac{\pi^2}{3} k_B^2 T p \cdot \left|\frac{AE_F}{\Gamma_E}\right|^{p-1} \cdot \frac{A}{\Gamma_E}. \quad (8)$$

This formula gives a good fit for moderate p values, as shown in Fig. 3(a), but does fail in the limit of $p \leq 1$ due to the $p - 1$ term in the exponent of the Fermi level. Equation 8 gives an expression relating S and E_F, and we can once again use the strategy described earlier to find S vs σ for high n.

As seen in Fig. 3(b), at high carrier concentrations, the mobility saturates and becomes somewhat independent of n. Because of this, we can take mobility as a constant dependent only on the normalized energetic disorder $\widehat{\Gamma} = \Gamma_E/kT$ and the mobility at $1kT$ of disorder (μ_{1kT}) such that $\mu_{\text{sat}} = \frac{\mu_{1kT}}{\widehat{\Gamma}}$, as shown in Fig. 3(c). This relationship is surprisingly simple—a polymer achieves its maximum mobility in the disorderless limit, $\Gamma_E = 1kT$, relatively independent of the p value. This disorderless limit of mobility μ_{1kT} is material dependent and contains all the effects besides energetic disorder, such as positional disorder, partial carrier

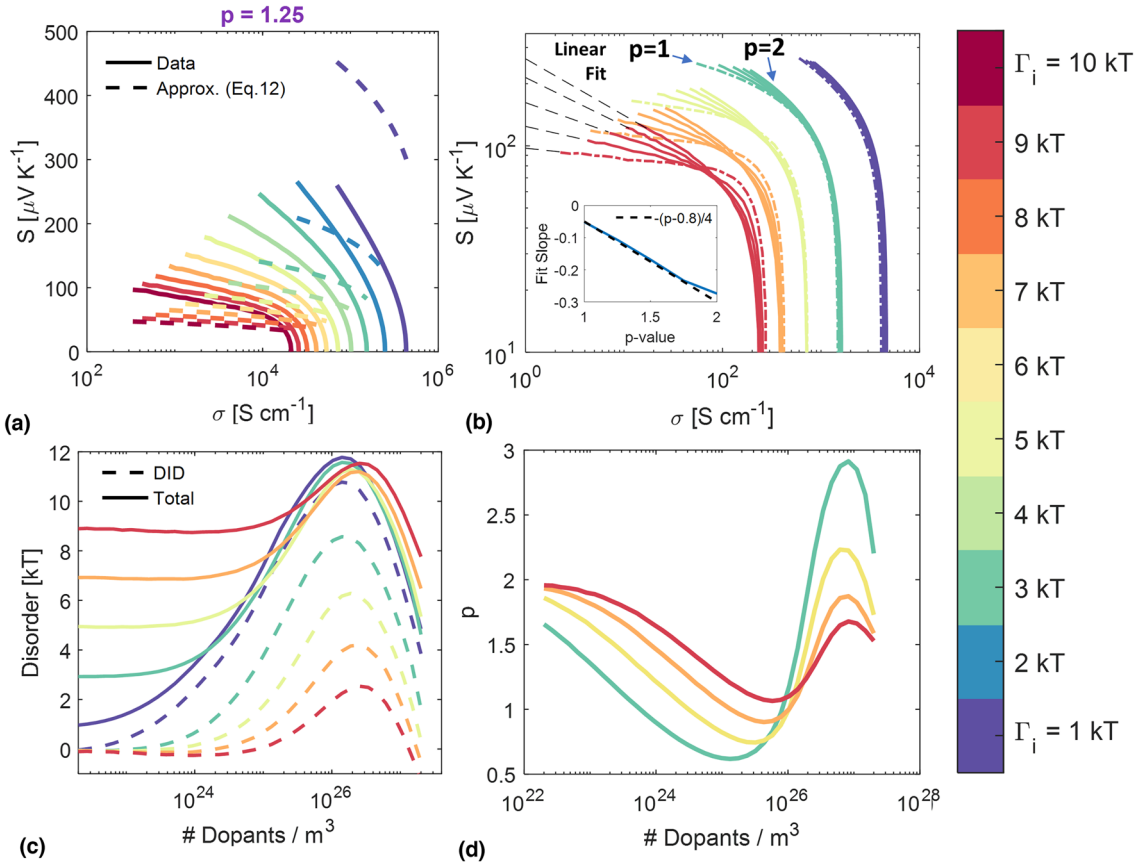

Figure 4. (a) Solid lines are hopping transport results while dashed lines depict Eq. 10, our approximation of $S(\sigma)$. The approximation fails at p = 1.0 due to the $p-1$ term inherited from the Mott formula, but it shows good agreement above $\Gamma_E = 3kT$, in the range of most polymers. (b) Plotting all S vs σ curves across p and Γ_E, we see that at high doping the maximum conductivity is dictated by the energetic disorder, and at high energetic disorders the slope is controlled by the p value, with a flatter slope for lower p values. (c) The energetic and dopant-induced disorders are shown as a function of the number of dopants. The total disorder reaches a common peak with doping, upon which further doping decreases the disorder through disorder compensation. (d) The p value is shown as a function of the number of dopants. p starts near 2 and decreases with doping, but then seems to increase back to 2 or even higher at high doping.

delocalization, overlap between the wavefunctions of neighboring states, and the phonon-assisted attempt-to-hop rate. The saturation mobility is inversely proportional to the normalized energetic disorder and describes the maximum achievable mobility for a polymer having a given energetic disorder. Additionally, this means that the maximum achievable conductivity for a polymer is dictated solely by Γ_E and nearly independent of the DOS shape parameter p because $\sigma_{sat} = q\mu_{sat}N_0 = q\mu_{1kT}N_0\left(\frac{k_BT}{\Gamma_E}\right)$ which is shown as follows.

Next, to find $E_F(\sigma)$, we reuse Eq. 4—the relationship between E_F and n for low n—and use $\sigma = q\mu n$, where μ is now set equal to μ_{sat}. We obtain

$$E_F \propto \gamma k_B T ln\left(\frac{\sigma}{\sigma_{sat}}\right), \tag{9}$$

where the E_F vs σ curves are no longer parallel but instead proportional to γ. The performance of Eq. 9 is surprisingly good, as Eq. 4 underpredicts the slope of $E_F(n)$ at high n, but Eq. 9 describes the slope of $E_F(\sigma)$ well, as shown in Fig. 3(d). A more detailed discussion of Eq. 9 is given in the Supplemental Information, Sect. S4.

Finally, to establish a relationship between S and σ for high n, we combine Eqs. 8 and 9 to find

$$S \approx \frac{\pi^2}{3}\frac{k_B}{q}p\left(\frac{A}{\widehat{\Gamma}}\right)^p \gamma^{p-1}\left[ln\left(\frac{\sigma_{sat}}{\sigma}\right)\right]^{p-1}. \tag{10}$$

This equation gives a qualitative fit of the data as shown in Fig. 4(a). Equation 10 shows us that unlike at low n, the slope of S vs σ at high n is heavily affected by both the Γ_E and p values. The term $p\left(\frac{A}{\widehat{\Gamma}}\right)^p \gamma^{p-1}$ controls the slope of the curve, which decreases with Γ_E and increases with p, and the $p-1$ exponent to $\ln\left(\frac{\sigma_{sat}}{\sigma}\right)$ controls the curvature. For large values of σ approaching σ_{sat}, the logarithm is approximately linear, such that our equation shows $S \propto \sigma^{-(p-1)}$. From this, we would relate the DOS shape parameter to the Kang-Snyder exponent via $s \approx 1/(p-1)$. We examine the relationship between the slope of S vs σ and the DOS shape parameter p value more closely in Fig. 4(b), with the inset

showing that p can be related to the Kang-Snyder exponent more accurately through $s = 4/(p - 0.8)$. A purely Gaussian DOS (p = 2) would correspond to s ≈ 3.33 while s = 4 and 8 map closely to p = 1.75 and 1.25, respectively. Therefore, a higher exponent corresponds to a more heavy-tailed DOS.

These effects can be seen quite clearly by looking at the S vs σ curves across all Γ_E and p values as shown in Fig. 4(b). Here, we see again that the maximum conductivity σ_{sat} is controlled almost entirely by the energetic disorder and independent of the p value, as predicted previously, so that lower Γ_E consistently gives a higher conductivity and a higher power factor. The slope of S vs σ becomes flatter and more p dependent as Γ_E increases, with a larger p giving a steeper slope. Above $\sim 5k_BT$ of energetic disorder, there is a crossover point where S vs σ at $p = 1$ is greater than at $p = 2$ at the highest conductivities, such that the power factor is higher for $p = 1$. This means that at low energetic disorder, a high p value is desirable, but at high energetic disorder, it is favorable to have a lower p value. The power factor is plotted for these same values in Fig. S5 of the Supplemental Information.

Lastly, we turn our attention to the amount of DID as a function of doping. Figure 4(c) shows the energetic disorder as function of doping, extracted from the standard deviation of the DOS computed from the Arkhipov model, as described in Methods. The total energetic disorder increases to a maximum that is largely independent of the intrinsic disorder, then decreases due to disorder compensation.[19] Carrier screening can also impact the energetic disorder at high doping.[20] We also note that the amount of DID is greater when the intrinsic energetic disorder is small. However, the total energetic disorder for all cases is above $5k_BT$ at high doping, implying that most doped polymers are in a range where the slope of the $S - \sigma$ curve is controlled by the p value.

Figure 4(d) shows the p value as a function of doping. We observe that DID reduces the p value from the initial value of $p = 2$, which indicates a gaussian intrinsic DOS, to values around 1, indicative of a heavy exponential tail. The amount of reduction in p value is greater if the intrinsic energetic disorder is small—if we start out with a narrow DOS, then DID will affect it more by creating a pronounced tail. On the other hand, when the intrinsic DOS is a wide gaussian, the tail is less pronounced, and the DOS retains its gaussian shape. Consequently, polymers with lower intrinsic disorder will have a lower p value, resulting in a flatter slope of the S vs σ curve, as was shown in our earlier work[5] and confirmed in Supplemental Fig. S6. Ultimately, at high doping, the p value recovers back up to and above the initial value of $p = 2$, reaching higher p values for higher intrinsic disorders, but this occurs at very high doping concentrations where the Seebeck coefficient begins to abruptly decrease as the Fermi level reaches the flat top of the DOS.

Conclusion

We have carefully analyzed the impacts of carrier concentration, the width, and the shape of the electronic DOS on transport and the S vs σ curve. We find distinct S vs σ behavior at low vs high carrier concentrations n. At low n, the transport energy is independent of n and far from the Fermi level. We show the $E_F(n)$ and $\sigma(n)$ curves have a Γ_E and p dependence, with their slope depending on the parameter $\gamma(\Gamma_E, p)$, such that the dependence cancels and the slope of E_F vs σ is constant, producing a universal S vs σ slope of $-k_B/q$. At high n, where the Fermi level and transport energy are close and nearly parallel, the mobility μ saturates to a nearly constant value μ_{sat} such that $\sigma \propto \gamma E_F$ and the S vs σ slopes are no longer constant but instead have a Γ_E and p dependence. We show that the Mott Formula works qualitatively well here, allowing us to derive an expression capturing the Γ_E and p dependence of the slope. We also show that a polymer's maximum attainable conductivity is inversely proportional to the energetic disorder but largely independent of DOS shape parameter.

It is important to note that the equations we derive in this paper describe S vs σ for a fixed DOS at a specific carrier concentration. When doping a polymer, the shape of the DOS evolves with doping. Deriving analytical expressions for $\Gamma_E(n)$ and $p(n)$ could allow us to describe the evolution of the S vs σ curve in a system with DID, but it is left for future work. Instead, we correlate both energetic disorder and the DOS shape to doping via the Arkhipov model and find that, at high carrier concentrations, the S vs σ curve is highly p dependent, such that low p produces a higher power factor. Thus, finding ways to maintain a low p value could increase the maximum efficiency of heavily doped thermoelectrics. One way this may be achieved is by starting from a polymer with very low intrinsic energetic disorder, which produces a heavier tail and flatter S vs σ curve but may result in higher power factors. We believe that by providing an understanding for the underlying effects of carrier injection and the DOS shape on the S vs σ curve, we may better mitigate the S vs σ tradeoff and find better thermoelectric materials.

Author contributions

A.T. performed the calculations, plotted the figures, and drafted the manuscript. Z.A. conceived the idea, wrote the simulation code, and edited the manuscript. The authors analyzed results and finalized the manuscript collaboratively.

Funding

This work was supported by the National Science Foundation's Division of Materials Research through Grant Number DMR-2101127.

Data availability

All data in this manuscript are available from the corresponding author on reasonable request.

Declarations

Conflict of interest

This work has no conflicts of interest.

Supplementary Information

The online version contains supplementary material available at https://doi.org/10.1557/s43579-024-00628-2.

References

1. G.H. Kim, L. Shao, K. Zhang, K.P. Pipe, Engineered doping of organic semiconductors for enhanced thermoelectric efficiency. Nat. Mater. **12**(8), 719–723 (2013). https://doi.org/10.1038/nmat3635
2. O. Bubnova, X. Crispin, Towards polymer-based organic thermoelectric generators. Energy Environ. Sci. **5**(11), 9345–9362 (2012). https://doi.org/10.1039/c2ee22777k
3. O. Bubnova et al., Optimization of the thermoelectric figure of merit in the conducting polymer poly(3,4-ethylenedioxythiophene). Nat. Mater. **10**(6), 429–433 (2011). https://doi.org/10.1038/nmat3012
4. P. Kar, *Doping in conjugated polymers* (Wiley, Hoboken, 2013)
5. M. Upadhyaya et al., Raising dielectric permittivity mitigates dopant-induced disorder in conjugated polymers. Adv. Sci. (2021). https://doi.org/10.1002/advs.202101087
6. H. Li et al., Dopant-dependent increase in Seebeck coefficient and electrical conductivity in blended polymers with offset carrier energies. Adv. Electron. Mater. (2019). https://doi.org/10.1002/aelm.201800618
7. Y. Xuan et al., Thermoelectric properties of conducting polymers: the case of poly(3-hexylthiophene). Phys. Rev. B (2010). https://doi.org/10.1103/PhysRevB.82.115454
8. H. Abdalla, G. Zuo, M. Kemerink, Range and energetics of charge hopping in organic semiconductors. Phys. Rev. B (2017). https://doi.org/10.1103/PhysRevB.96.241202
9. A.M. Glaudell, J.E. Cochran, S.N. Patel, M.L. Chabinyc, Impact of the doping method on conductivity and thermopower in semiconducting polythiophenes. Adv. Energy Mater. (2015). https://doi.org/10.1002/aenm.201401072
10. S. Dongmin Kang, G. Jeffrey Snyder, Charge-transport model for conducting polymers. Nat. Mater. **16**(2), 252–257 (2017). https://doi.org/10.1038/nmat4784
11. C.J. Boyle et al., Tuning charge transport dynamics via clustering of doping in organic semiconductor thin films. Nat. Commun. (2019). https://doi.org/10.1038/s41467-019-10567-5
12. H. Tanaka et al., Thermoelectric properties of a semicrystalline polymer doped beyond the insulator-to-metal transition by electrolyte gating. Sci. Adv. **6**, 8065–8079 (2020). https://doi.org/10.1126/sciadv.aay8065
13. M. Upadhyaya, C.J. Boyle, D. Venkataraman, Z. Aksamija, Effects of disorder on thermoelectric properties of semiconducting polymers. Sci. Rep. (2019). https://doi.org/10.1038/s41598-019-42265-z
14. A.A. Roenko, V.V. Lukin, I. Djurovič, M. Simeunovič, Estimation of parameters for generalized Gaussian distribution. IEEE Xplore (2014). https://doi.org/10.1109/ISCCSP.2014.6877892
15. F. Zhang et al., Modulated thermoelectric properties of organic semiconductors using field-effect transistors. Adv. Funct. Mater. **25**(20), 3004–3012 (2015). https://doi.org/10.1002/adfm.201404397
16. C.N. Warwick, D. Venkateshvaran, H. Sirringhaus, Accurate on-chip measurement of the Seebeck coefficient of high mobility small molecule organic semiconductors. APL Mater. (2015). https://doi.org/10.1063/1.4931750
17. D. Venkateshvaran et al., Approaching disorder-free transport in high-mobility conjugated polymers. Nature **515**(7527), 384–388 (2014). https://doi.org/10.1038/nature13854
18. M. Jonson, G.D. Mahan, Mott's formula for the thermopower and the Wiedemann-Franz law. Phys. Rev. B **21**(10), 4223–4229 (1980)
19. A. Fediai, F. Symalla, P. Friederich, W. Wenzel, Disorder compensation controls doping efficiency in organic semiconductors. Nat. Commun. (2019). https://doi.org/10.1038/s41467-019-12526-6
20. M. Duhandžić, M. Lu-Dìaz, S. Samanta, D. Venkataraman, Z. Akšamija, Carrier screening controls transport in conjugated polymers at high doping concentrations. Phys. Rev. Lett. (2023). https://doi.org/10.1103/PhysRevLett.131.248101